ADAPTIVE METHOD OF LINES TECHNIQUES FOR VAPOR INFILTRATION PROBLEMS

S. Adjerid, J. E. Flaherty, W. Hillig, J. Hudson, and M. S. Shephard

Scientific Computation Research Center
and
Center for Composite Materials and Structures

Rensselaer Polytechnic Institute, Troy, New York 12180, USA
Tel: 518-276-6348 / Fax: 518-276-4033 / e-mail: flaherje@cs.rpi.edu

1. Introduction

Patibandla et al. [4,5] describe a reactive vapor infiltration (RVI) process for manufacturing fiber-reinforced ceramic composites where silicon carbide (SiC) or alumina (Al_2O_3) fibers are mixed with molybdenum (Mo) powder and pressed at room temperature to form a porous preform. The preform is exposed to a silicon tetra-chloride ($SiCl_4$) and hydrogen (H_2) flow where molecular-surface reactions liberate Si which, when absorbed into the preform, reacts with Mo to form a molybdenum di-silicide ($MoSi_2$) matrix. As a first step in modeling the RVI process, we present a mathematical model of the diffusion of Si into a compressed-powder Mo pellet to form the $MoSi_2$ matrix. The production of an intermediate (Mo_5Si_3) silicide layer, the growth of the $MoSi_2$ layer, and the volume expansion of the pellet are predicted. The resulting partial differential system is solved using an adaptive software system [2] that includes capabilities for automatic quadtree-structured mesh generation, mesh refinement/coarsening (h-refinement), method order variation (p-refinement), and mesh motion (r-refinement). Computational solutions of one- and two-dimensional problems indicate that the adaptive software is a robust and effective tool for addressing composite-processing problems. The mathematical model predicts the observed parabolic growth rate of the silicide layer and the volume expansion of the pellet to a high degree of accuracy.

2. RVI Model

The loosely compacted pellet is subjected in a furnace to a flow of $SiCl_4$ and H_2 that reacts on the surface of grains of the pellet to liberate Si [4,5]. The Si is absorbed into the Mo pellet and reacts as

$$5Mo + 3Si \xrightarrow{k_1} Mo_5Si_3, \quad Mo_5Si_3 + 7Si \xrightarrow{k_2} 5MoSi_2 \tag{2.1}$$

to form Mo_5Si_3 and the desired $MoSi_2$ silicide. These reactions occur in narrow fronts with free Si diffusing (principally by solid-state diffusion) through an $MoSi_2$ layer to reach the reaction zones. The reactions (2.1) are accompanied by a 158% volume increase which fills the pores between grains of Mo powder, but may cause cracking [4,5].

Suppose the pellet contains a mixture of reactants and products and let the mass m_i (g) of species i at time t in a control volume V be

$$m_i = \int_V \rho Y_i \, dV, \quad i = 1, 2, 3, 4, \tag{2.2}$$

where ρ (g/cm^3) is the mixture density and Y_i, $i = 1, 2, 3, 4$, are, respectively, the mass fractions of Si, $MoSi_2$, Mo_5Si_3, and Mo. As the pellet deforms due to the volume change, we specify the position of each material point $\mathbf{x}$ as a function of t and its initial spatial position $\mathbf{X}$. With this reference, considerations of mass conservation for species i imply that

$$\frac{dm_i}{dt} = -\int_{\partial V} \mathbf{J}_i \cdot \mathbf{n} \, d\sigma - \int_{\partial V} \rho Y_i \mathbf{v} \cdot n \, d\sigma + \int_V \dot{r}_i \, dV, \quad i = 1, 2, 3, 4, \tag{2.3}$$

where ∂V, with unit outer normal $\mathbf{n}$, is the boundary of V; $\mathbf{v}(\mathbf{X},t) = \partial_t \mathbf{x}(\mathbf{X},t)$ (cm/sec) is the mixture velocity; and $\dot{r}_i$ $(g/cm^3/sec)$ is the mass production rate and $\mathbf{J}_i$ $(g/cm^2/sec)$ is the diffusive flux of species i. Assuming Fickian diffusion $\mathbf{J}_i = -D_i \nabla(\rho Y_i)$, with D_i (cm^2/sec) being the diffusivity of species i in the mixture.

Applying the divergence theorem to (2.3) and using (2.2) yields the partial differential system

$$\frac{D(\rho Y_i)}{Dt} = \partial_t(\rho Y_i) + \mathbf{v} \cdot \nabla(\rho Y_i) = \nabla \cdot D_i \nabla(\rho Y_i) - \rho Y_i \nabla \cdot \mathbf{v} + \dot{r}_i, \quad \mathbf{x} \in \Omega, \quad t > 0, \quad i = 1, 2, 3, 4, \tag{2.4}$$

where Ω is the spatial region occupied by the pellet at time t.

Mass production rates are much faster than diffusion rates and, thus, cannot be observed. We assume that all reactions are irreversible, isothermal, cease when one or more reactants are depleted, and are linear in each concentration to obtain

$$\dot{r}_1 = -M_1(3w_1 + 7w_2), \quad \dot{r}_2 = 5M_2w_2, \quad \dot{r}_3 = M_3(w_1 - w_2), \tag{2.5a,b,c}$$

$$\dot{r}_4 = -5M_4w_1, \quad w_1 = k_1(\frac{\rho Y_1}{M_1})(\frac{\rho Y_4}{M_4}), \quad w_2 = k_2(\frac{\rho Y_1}{M_1})(\frac{\rho Y_3}{M_3}). \tag{2.5c,d,e}$$

The variables k_1 and k_2 (cm^3/sec) identify the rates of the reactions (2.1) and M_i (g) denotes the molecular weight of species $i = 1, 2, 3, 4$ [3].

To include expansion, consider a volume V at time t where each chemical occupies the portion V_i, $i = 1, 2, 3, 4$. Letting V_0 denote the volume of the voids between chemical compounds, $v(\mathbf{x},t) = V_0/V$ denote the porosity, $\hat{\rho}_i = m_i/V_i$ (g/cm^3), $i = 1, 2, 3, 4$, denote species densities [3], using (2.2), and letting V tend to zero gives

$$1 - v = \sum_{i=0}^{4} \frac{V_i}{V} = \sum_{i=1}^{4} \frac{m_i}{\hat{\rho}_i V} = \sum_{i=1}^{4} \frac{1}{\hat{\rho}_i V} \int_V \rho Y_i \, dV = \sum_{i=1}^{4} \frac{\rho Y_i}{\hat{\rho}_i}. \tag{2.6}$$

Multiplying (2.4) by $1/\hat{\rho}_i$, summing over i, and using (2.6), we obtain

$$-\frac{Dv}{Dt} + (\nabla\cdot\mathbf{v})(1 - v) = \sum_{i=1}^{4} \frac{1}{\hat{\rho}_i}[\dot{r}_i + \nabla\cdot D_i\nabla\rho Y_i], \quad \mathbf{x}\in\Omega, \quad t > 0. \tag{2.7}$$

We simplify (2.7) by including the effects of v in the densities of the mixture components. With little free *Si* in the pellet, it is reasonable to neglect V_1/V. Furthermore, the diffusivities D_i, $i = 2, 3, 4$, are negligible relative to D_1. Thus, all diffusive terms are neglected, and we approximate (2.7) as

$$\nabla\cdot\mathbf{v} = \sum_{i=2}^{4} \frac{\dot{r}_i}{\hat{\rho}_i}. \tag{2.8}$$

The system is closed by the mixture momentum equation for a viscous medium

$$\rho\frac{D\mathbf{v}}{Dt} + \mathbf{v}[\partial_t\rho + \nabla\cdot(\rho\mathbf{v})] = \nabla\cdot\mathbf{T} \tag{2.9a}$$

where the traction matrix $\mathbf{T}$ (Pa) has components

$$T_{i,j} = (-p + \lambda\nabla\cdot\mathbf{v})\delta_{i,j} + \mu(\partial_{x_j}v_i + \partial_{x_i}v_j) \tag{2.9b}$$

with λ and μ being Lamé parameters, p (Pa) being the pressure, and $\delta_{i,j}$ being the Kronecker delta.

Specification of initial and boundary conditions complete the model (2.4,5,8,9). When only *Mo* powder is present in the initial state, we prescribe

$$\rho(\mathbf{X},0) = \bar{\rho}, \quad Y_i(\mathbf{X},0) = 0, \quad i = 1, 2, 3, \quad Y_4(\mathbf{X},0) = 1, \quad v(\mathbf{X},0) = 0, \quad \mathbf{X}\in\Omega\cup\partial\Omega, \tag{2.10}$$

where $\bar{\rho}$ is the initial mixture density. Boundary conditions are developed by assuming that the reaction at the surface of the pellet ceases when a full monolayer of *Si* atoms is present on the surface. Therefore, the flux of *Si* atoms being absorbed into the pellet must equal the rate at which they are produced by this reaction. Moreover, we assume that the rate of absorption of *Si* atoms is proportional the deviation of Y_1 from twice the maximum solubility S of *Si* in $MoSi_2$. Boundary fluxes of other species are neglected; thus,

$$D_1\nabla(\rho Y_1)\cdot\mathbf{n} = -\alpha(Y_1 - S), \quad D_i\nabla(\rho Y_i)\cdot\mathbf{n} = 0, \quad i = 2, 3, 4, \quad \mathbf{x}\in\partial\Omega, \quad t > 0. \tag{2.11}$$

3. Computational Results

We use an adaptive finite element software system with capabilities for automatic h-, p-, and/or r-refinement [3] to solve dimensionless versions of (2.4,5,8,9,11,12) in one and two spatial dimensions. With mesh motion, for example, we can both follow evolving fronts and track the volume expansion as the reaction progresses. The particular combination of h- and p-refinement is remarkably effective when high accuracy is necessary. Mesh refinement and order variation are controlled by a posteriori estimates of local discretization errors [2] or error indicators. Herein, error indicators involved jumps in the computed flux across element boundaries [2,3].

With the origin of a Cartesian coordinate system at the center of a $2a\times2b\times2c$ pellet, we introduce dimensionless variables with (x_1,x_2,x_3) scaled by (a,b,c), t scaled by $M_4/k_1\bar{\rho}$, and ρ scaled by $\bar{\rho}$. Employing symmetry, one-dimensional problems are solved on $0 < x_1 < a$ with x_2 and x_3 derivatives set to zero. The initial *Mo* pellet has a 45% porosity with $a = 1$ (mm), $\alpha = 10^6$ $(g/cm^2/sec)$, $S = 0.00037$, $k_1 = 1.5\times10^3$ and $k_2 = 1.5\times10^2$ (g/cm^3),

$D_1 = 0.37\times10^{-5}$, 1.5×10^{-5}, and 4.2×10^{-5} (cm^2/sec), and $D_i = 10^{-20}$ (cm^2/sec), $i = 2, 3, 4$. The three values of D_1 correspond to observed diffusivities of Si at, respectively, temperatures of 1100, 1200, and 1300 $(°C)$ [3-5].

We compare computed and observed [4,5] results for the square of the thickness of the $MoSi_2$ layer as a function of time for three temperatures in the left portion of Figure 1. Computed and experimental results are in excellent agreement with deviations being less than 10%. Mass concentrations of $MoSi_2$, Mo_5Si_3, and Mo at a temperature of 1200 $°C$ and $t = 9.2$ hr are shown as a function of position in the right portion of Figure 1. The $MoSi_2$ layer is progressing from right to left in Figure 2; thus, the right-most curve is the mass fraction of $MoSi_2$, the steeply-peaked center curve is the mass fraction of Mo_5Si_3, and the left-most curve is the unreacted Mo.

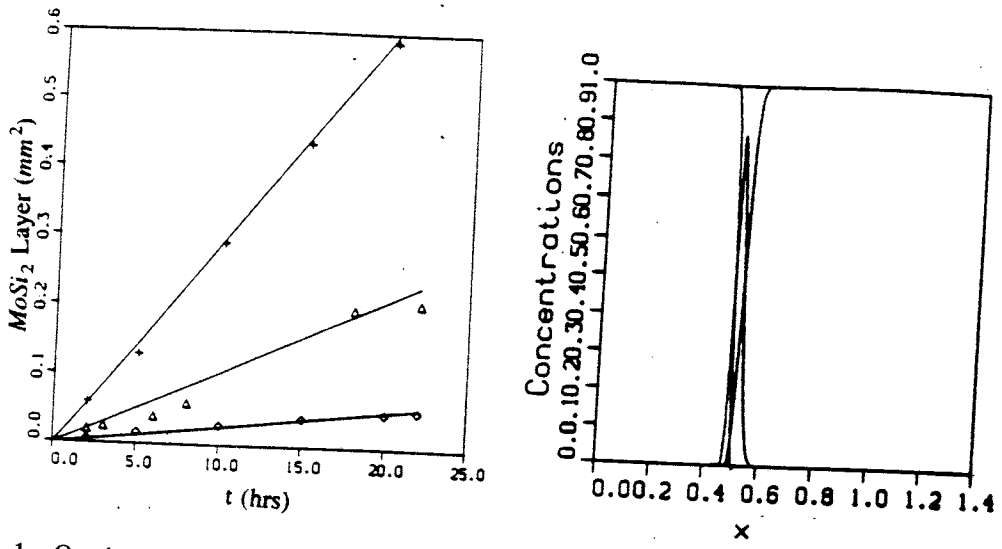

Figure 1. On the left, comparison of computed and observed values of the square of the thickness of the $MoSi_2$ layer as a function of time for temperatures of 1100 $°C$ (diamonds), 1200 $°C$ (triangles), and 1300 $°C$ (plusses). On the right, mass fractions of $MoSi_2$, Mo_5Si_3, and Mo at 1200 $°C$ and $t = 9.2$ hr as a function of position.

Solutions shown in Figure 1 were obtained by hpr-refinement and in the left portion of Figure 2 we show the spatial mesh and method order used at 1200 $°C$ and $t = 9.2$ hr. A coarse mesh and first-order method are used away from the reaction zone while finer meshes and high-order methods are used near the reaction. The mesh used to solve this problem is shown as a function of time in the right portion of Figure 3. The mesh is concentrated near the front and moving to account for the expansion as the reaction occurs.

We also solved a two-dimensional problem involving a $a = 1\times10$ (mm^2) pellet with the parameters as specified for the one-dimensional problem at 1200 $°C$. In Figure 3, we show a quadrant of the mesh at 2, 10, and 30 hrs. obtained using piecewise-bilinear finite element approximations with Lobatto quadrature used to eliminate spurious oscillations [1]. Expansion occurs in regions having high $MoSi_2$ concentrations.

4. Discussion

We have developed a reaction-diffusion system to analyze the RVI and other chemical vapor infiltration processes of fabricating ceramic composites. When used with an adaptive finite element software system [2], the model predicted the growth of an $MoSi_2$ layer in a siliciding application [4,5]. Production rates, volume expansion, residual stresses and other effects may be studied as functions of, e.g., initial composition, temperature, and porosity.

Future experiments will be performed with fibers embedded in a powder preform and our models will be modified to reflect this. Our investigation will seek to reveal optimal fiber placements, packing densities, and process strategies. By combining a computational and experimental program we are able to identify and verify prototypical optimal combinations much more rapidly than would be possible by using either paradigm alone.

5. Acknowledgment

This research was supported by ARPA/ONR under grant N00014-92J-1779 and by AFOSR under grant F49620-93-1-0218.

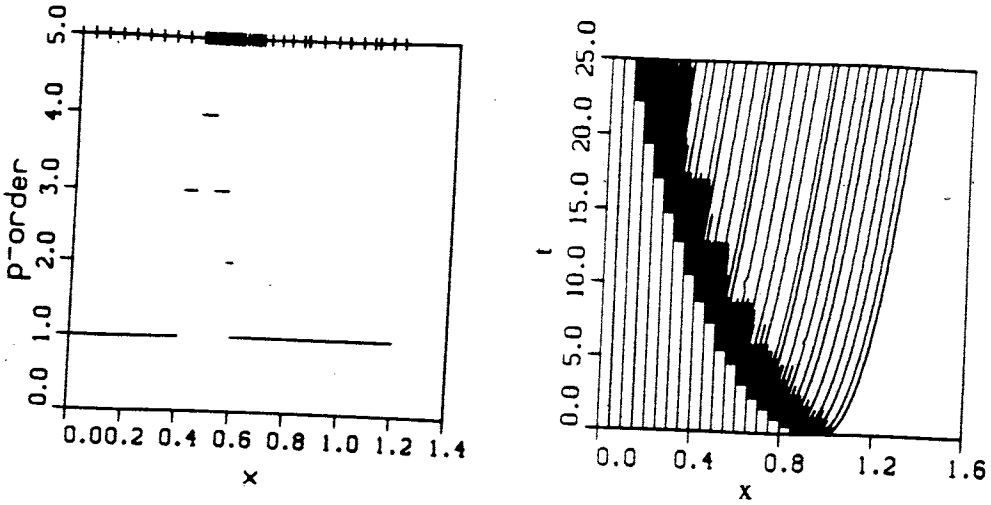

Figure 2. Method order and spatial mesh (left) and mesh position as a function of time (right).

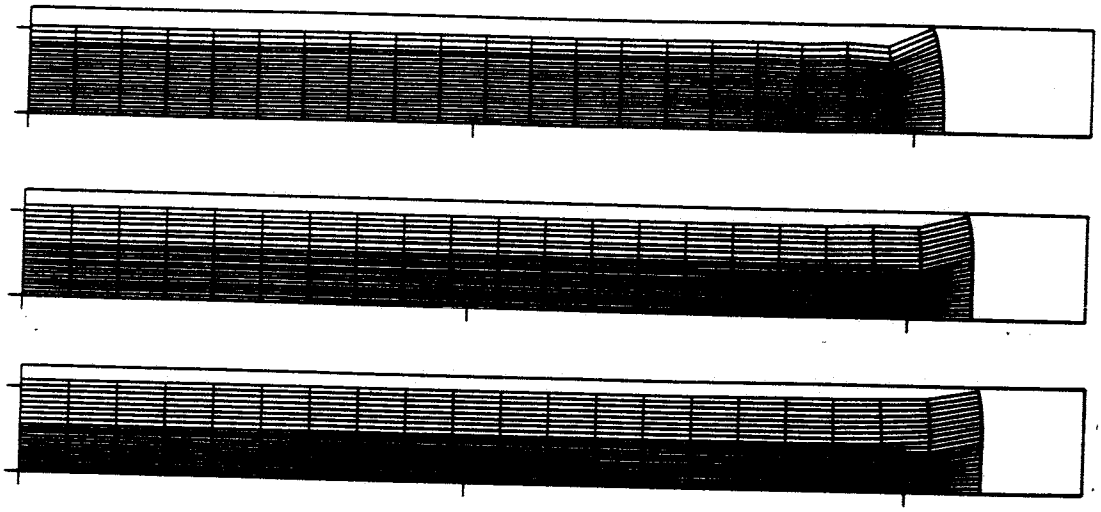

Figure 3. Meshes at 2 (top), 10 (center), and 30 (bottom) hrs. for a two-dimensional pellet.

6. References

1. S. Adjerid, M. Aiffa, and J.E. Flaherty, High-Order Finite Element Methods for Singularly-Perturbed Elliptic and Parabolic Problems, *SIAM J. Appl. Math.*, to appear, 1994.

2. S. Adjerid, J.E. Flaherty, P.K. Moore, and Y.J. Wang, High-Order Methods for Parabolic systems, *Physica D*, Vol. 60, pp. 94-111, 1992.

3. S. Adjerid, J.E. Flaherty, M.S. Shephard, Y.J. Wang, W. Hillig, J. Hudson, and N. Patibandla, SCREC Rep. #2-1994, Sci. Comp. Res. Ctr., Rensselaer Polytech. Inst., 1994

4. N. Patibandla and W.B. Hillig, Processing of Molybdenum Di-silicide Using a New Reactive Vapor Infiltration Technique, *J. Am. Ceram. Soc.*, Vol. 76, pp. 1630-1634, 1993.

5. N. Patibandla, W.B. Hillig, and M.R. Ramakrishnan, *SiC* Fiber Reinforced $MoSi_2$ Matrix Composites Produced Via Reactive Vapor Infiltration, preprint, Cent. Compos. Mat'ls. and Struct., Rensselaer Polytech. Inst., 1993.